INFLUENCE OF DIMENSIONS AND DENSITY OF WATER TREES ON RESIDUAL ELECTRIC FIELD IN POLYMERIC POWER CABLES INSULATIONS

CRISTINA STANCU[1], PETRU V. NOŢINGHER[2], CONSTANTIN STOICA[2], MIHAI PLOPEANU[2], PETRU NOŢINGHER JR.[3]

Key words: Cable insulation, Electric field, Space charge, Water treeing.

In this paper, the residual electric field computation in a cable insulation in the presence of water trees and space charge is presented. Considering that, in treed areas, the variations of the permittivity and the space charge density are known, the thermal step current $I_c(t)$ is computed and the curves $I_m(t)$ and $I_c(t)$ are compared. The results show an important increase of residual electric field for some dimensions and concentrations of the water trees (up to 10 MV/m). Finally, the influence of the residual electric field on electrically aged cable insulations is analyzed.

1. INTRODUCTION

Use of the thermoplastic polymers (polyethylene, polyvinyl chloride, ethylene propylene rubber) in power cables insulations presents important advantages due to technical and technological properties superior to those of paper and oil, respectively superior mechanical properties, higher operating temperature, easier maintenance and replacement etc. In a series of papers it is shown that, in polyethylene insulations, water trees appear (Fig. 1) and their inception and development is due to existence of ions inside water contained by polymers (and/or which comes into contact with them) and a time variable electric field [1–2]. Water trees can be presented in all of the medium voltage cables, manufactured in 70–80's and which are not provided with polyethylene protection jacket.

Studies made on low density and crosslinked polyethylene showed positive and negative ions existence, both inside and outside of trees, and constitute ionic space charge [2–3]. The space charge generates an electric field, which overlaps on the existing one, leading to the electric field enhancement outside of treed areas and to the increase of insulation premature breakdown probability.

Furthermore, after the voltage switching-off, the space charge remains inside and in vicinity of treed areas, and the insulation presents a residual electric field for a long time after the voltage is removed [3]. Since residual electric field facilitates

Rev. Roum. Sci. Techn. – Électrotechn. et Énerg., **55**, *3*, p. 289–299, Bucarest, 2010

the processes of the insulation electrical degradation, knowing its values is very important.

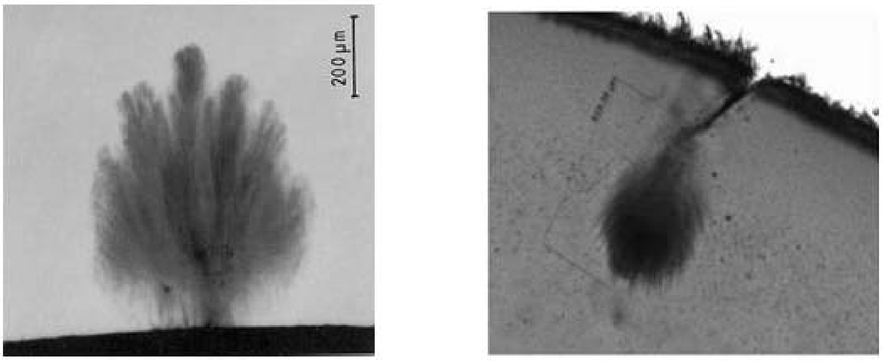

a) b)

Fig. 1 – Vented trees in polyethylene insulation of a cable, developed on inner (a) and outer (b) semiconductor layer.

The space charge can be easily determined in homogeneous insulations by measuring the thermal step current and by using a relative simple relation [4–5]. In the case of inhomogeneous insulations (with water trees), the use of this method becomes more complicated, because the insulation permittivity varies in the treed areas.

In previous papers [4–8], some aspects regarding the electric field computation in cable insulations in service (in the absence and presence of water trees) have been presented. In this paper, a computation method of residual electric field in medium voltage cables in the presence of water trees obtained by accelerated electrical ageing on the basis of thermal step current is presented. Also, the influence of concentrations and dimensions of water trees on the potential values, residual electric field and insulation electrical degradation is analyzed.

2. EXPERIMENTS

2.1. SAMPLES

In order to obtain water trees with different dimensions and concentrations, accelerated ageing tests on crosslinked polyethylene minicables (having the outer radius of inner semiconductor r_i = 1.4 mm and the inner radius of outer semiconductor r_e = 2.9 mm (Fig. 2)) were made. The maximum applied field was E_{max} = 6 kV/mm and frequency f = 50 Hz, for τ = 200…1,000 h.

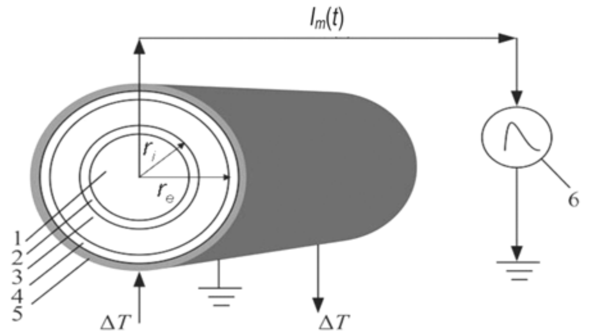

Fig. 2 – Diagram of thermal step method experimental set up on a cable sample: 1 – conductor; 2 – inner semiconductor; 3 – insulation; 4 – outer semiconductor; 5 – thermal diffuser; 6 – pico ammeter.

After ageing, on each sample, the thermal step current was measured and slices with 200 μm thickness were taken for trees analysis.

2.2. THERMAL STEP CURRENT MEASUREMENT

For thermal step current measurement on the tested samples, a thermal step of ΔT = 30 °C was applied using a thermal diffuser (5, Fig. 2) [5]. The measured current $I_m(t)$ (Fig. 2) is related to electric field $E(r)$ by the relation:

$$I(t) = -C\int_{r_i}^{r_e} \alpha(r)E(r)\frac{\partial T(r,t)}{\partial t}\,\mathrm{d}r, \tag{1}$$

where $\alpha = \alpha_d - \alpha_\varepsilon$ represents the difference between the thermal expansion coefficient α_d and the permittivity variation factor of insulation with temperature α_ε, C – sample capacity before the thermal step application, $E(r)$ – electric field strength in a coordinate point $r \in [r_i, r_e]$ and $T(r, t)$ – the temperature in the point of coordinate r at the instant t [9].

The temperature values $T(r,t)$ are obtained from the Fourier equation:

$$\gamma(r)c_p(r)\frac{\partial T(r,t)}{\partial t} = \mathrm{div}[(\lambda(r)\mathrm{grad}T(r,t))], \tag{2}$$

where $\gamma(r)$ represents the density, $c_p(r)$ the specific heat and $\lambda(r)$ the insulation thermal conductivity in the point of coordinate r.

The direct computation of electric field $E(r)$ using the equation (1) is very difficult, because the temperature matrix is badly conditioned. Therefore, in this paper, an iterative computation method (Ch. 3) is used. It is considered that space charge density $\rho_v(r)$ is known, the thermal step current $I_c(t)$ is calculated, the condition $I_c(t) = I_m(t)$ is verified and, finally, $E(r)$ is computed.

2.3. DIMENSIONS AND CONCENTRATIONS OF WATER TREES DETERMINATION

Determination of dimensions and concentrations of water trees were made using the setup from Figure 3. For each value of ageing time τ, several slices were taken from cables insulation and the number of trees N_w, length L_k and diameter D_k of each tree were determined. The average diameter D_m, length L_m and trees concentration c_{wtm} were computed using the expressions:

$$L_m = \frac{1}{N_w}\sum_{k=1}^{N_w} L_k ; \quad D_m = \frac{1}{N_w}\sum_{k=1}^{N_w} D_k ; \quad c_{wtm} = \frac{N_w}{2\pi r_i n}, \tag{3}$$

where n represents the number of taken slices.

Fig. 3 – Measurement of water trees dimensions
1 – sample; 2 – video camera; 3 – PC; 4 – monitor.

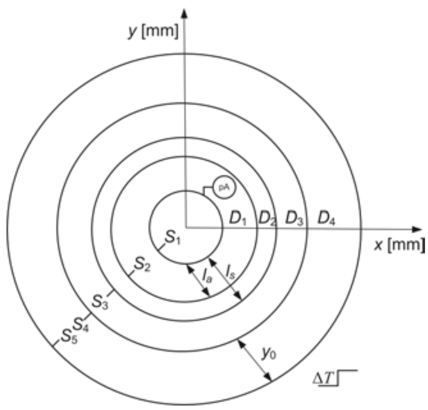

Fig. 4 – Computation domain of electric field.

3. ELECTRIC FIELD COMPUTATION

For electric field computation, it is considered that in cylindrical insulation of a cable (delimited by the cylindrical surfaces of radius r_i and r_e, Fig. 2) were developed – from inner surface S_1 – continuous trees (under the shape of cylindrical shell of thickness l_a) and an ionic space charge layer with the same shape and thickness $l_s > l_a$. As the electric field has a radial symmetry, for the computation it was considered a flat domain D, constituted from 4 sub-domains $D_{1\ldots4}$ delimited by the surfaces $S_1 \ldots S_5$ (Fig. 4):

– sub-domain D_1 (delimited by S_1 and S_2), corresponding to the water treed region of length l_a ($\varepsilon_r\,(r,\,T) = (1+\alpha_\varepsilon(T - T_0)\cdot c\mathrm{e}^{-dr})$) ($T_0$ is the temperature of the insulation before applying the thermal step). This region is supposed to contain a space charge layer of thickness l_a and of density $\rho_v(r) = \rho_{v0}(ar^2 + br + e)$;

– sub-domain D_2 (delimited by S_2 and S_3), with a space charge layer of thickness $l_s - l_a$ and of density $\rho_v(r) = \rho_{v0}(ar^2 + br + e)$;

– sub-domain D_3 (delimited by S_3 and S_4), without water trees and without space charge ($\varepsilon_r\,(T) = \varepsilon_{r\mathrm{PE}}(1+\alpha_\varepsilon(T - T_0))$);

– sub-domain D_4 (delimited by surfaces S_4 and S_5), corresponding to the region thermal diffuser/sample of thickness y_0, where the electric field is null.

The computation of the electric field and the temperature is done with the Comsol Multiphysics software, considering that y_0, l_a, l_s, a, b, e, $\alpha_{\varepsilon\mathrm{PE}}$, $\alpha_{\varepsilon w}$, c, c_1 d, d_1 and g as known and the Poisson $\Delta V = -\rho_v/\varepsilon$ and Fourier (eq. (2)) equations.

The boundary conditions are: $V(r) = 0$ on S_1, S_4 and S_5, $\overline{n}\left(\overline{D_1} - \overline{D_2}\right) = 0$ on S_2 and S_3, $T(r,\,t) = T_1$ on S_1, and $T(r,\,t) = T_5$ on S_5 (Figs. 3 and 4), where n is the normal to the surface, $\overline{D}$ – the electric displacement, T_1 and T_5 – the temperature values on the semiconductor layers surfaces (Fig. 3).

The material constants c and d from the expression of permittivity corresponding to D_1 ($\varepsilon_r(r) = c\mathrm{e}^{-dr}$) were determined with the expressions:

$$\varepsilon_r\left(r_i + l_a\right) = \varepsilon_{r\mathrm{PE}}\,; \quad \int_{r_i}^{r_i + l_a} \varepsilon_r(r)\mathrm{d}r = \varepsilon_{rm} l_a\,; \quad \varepsilon_{rm} = c_{wm}\varepsilon_{rm} + \left(1 - c_{wm}\right)\varepsilon_{r\mathrm{PE}}\,, \tag{4}$$

where c_{wm} represents the average water concentration in the water trees, ε_{rm} and $\varepsilon_{r\mathrm{PE}}$ are the relative permittivity of water and polyethylene and ε_{rm} is the average value of the permittivity in the water treed area (sub-domain D_1).

The values of α_ε were deduced on the basis of the permittivity variation curves for water and polyethylene at temperatures between $T_5 = -5$ °C and $T_1 = 25$ °C [10–11]. It was obtained $\alpha_{\varepsilon\mathrm{PE}} = 4.4 \cdot 10^{-4}\ \mathrm{K}^{-1}$ for polyethylene and $\alpha_{\varepsilon w} = -7.26 \cdot 10^{-3}\ \mathrm{K}^{-1}$ for water. Because the relative permittivity decreases exponentially with r, a variation law similar to the permittivity was considered for α_ε ($\alpha_\varepsilon(r) = c_1\mathrm{e}^{d_1 r}$). The values of c_1 and d_1 have been obtained from the following expressions:

$$\alpha_\varepsilon\left(r_i + l_a\right) = \alpha_{\varepsilon\mathrm{PE}}\,; \quad \int_{r_i}^{r_i + l_a} \alpha_\varepsilon(r)\mathrm{d}r = \alpha_{\varepsilon m} l_a\,; \quad \alpha_{\varepsilon m} = c_{wm}\alpha_{\varepsilon w} + \left(1 - c_{wm}\right)\alpha_{\varepsilon\mathrm{PE}}\,. \tag{5}$$

The average values of the quantities γ, λ, c_p, $\alpha_{\varepsilon m}$ and ε_{rm} for different values of the average water concentration c_{wm} are presented in Table 1.

Table 1

Values of material constants for different average water concentrations in polyethylene c_{wm} (l_a = 370 μm)

c_{wm} [%]	γ [kg/m^3]	λ [W/mK]	c_p [J/kgK]	$\alpha_{\varepsilon m}$ 10^4[K^{-1}]	ε_{rm}
0	930	0.38	1900	4.4	2.3
1	930.7	0.381	1923	3.63	3.1
2	931.4	0.409	2930	2.86	3.9

4. THERMAL STEP CURRENT COMPUTATION

Computed thermal step current $I_c(t)$ represents the time variation of charge Q_1 on the surface S_1 by the ionic space charge from insulation (domains D_1 and D_2) by applying thermal step ΔT [5], respectively:

$$I_c(t) \;=\; -\frac{\mathrm{d}Q_1}{\mathrm{d}t} = -2\pi r_i l \varepsilon_1 \frac{\dfrac{\mathrm{d}V}{\mathrm{d}x}\cdot\dfrac{\mathrm{d}^2V}{\mathrm{d}x\mathrm{d}t}+\dfrac{\mathrm{d}V}{\mathrm{d}y}\cdot\dfrac{\mathrm{d}^2V}{\mathrm{d}y\mathrm{d}t}}{\sqrt{\left(\dfrac{\mathrm{d}V}{\mathrm{d}x}\right)^2+\left(\dfrac{\mathrm{d}V}{\mathrm{d}y}\right)^2}}, \tag{6}$$

where $A_1 = 2\pi r_i l$ represents the area of the surface S_1, l – the length of the sample (l = 20 cm), ε_1 – the permittivity of the treed area and $V_1(x, y)$ – the electric potential corresponding to the space charge density $\rho_v(r)$ in the point $P(x, y)$ near S_1.

For the space charge density ρ_v a parabolic variation with the r coordinate was considered (in conformity with the experimental results presented in [3]):

$$\rho_v(r) = \rho_{v0}(ar^2 + br + e), \tag{7}$$

where ρ_{v0} is considered, at the beginning of the computation, to have values between 0.1 and 0.8 C/m^3, and $a = 4\cdot10^6$ m^{-2}, $b = -1.5$ m^{-1} and e = 14.44 [5].

5. RESULTS

In Fig. 5 the time variations of the measured thermal current (curves 1 and 3) and computed thermal step current (curve 2) are presented for two values of the electrical stress τ, 500 and 1,000 h. It can be observed that the increase of the ageing time leads to an increase in the values of the measured thermal step currents, their maximum values being 7.5 times greater than initial one when τ doubles.

The values for the dimensions (D_m and L_m) and for the average concentration (c_{wtm}) of the water trees in the samples on which the thermal step current was measured are presented in Table 2. As expected, the values of the three parameters

Table 2

Water trees dimensions and concentrations

Ageing time τ [h]	Average diameter D_m [μm]	Average length L_m [μm]	Average concentration c_{wtm} [mm^{-1}]
500	82.72	342.72	0.31
1000	109.77	370	1.27

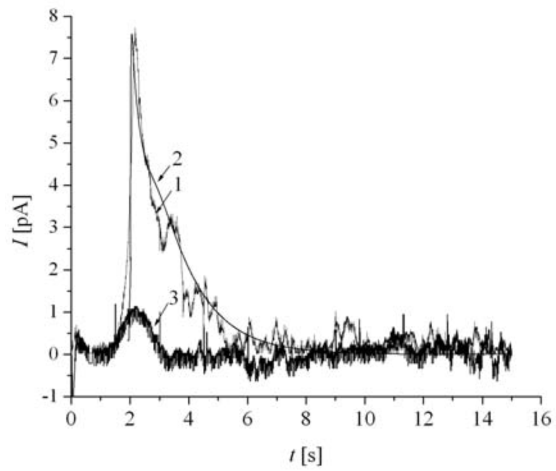

Fig. 5 – Variation with the time τ of the measured (1 and 3) and computed (2) thermal step current I, for τ = 1,000 h (1 and 2) and τ = 500 h (3).

increase with the electrical stress (phenomenon also observed in [8]). On the other hand, the increase of the number and dimensions of the water trees causes an increase in the values of the ionic space charge that leads to an increase in the values of both the measured and computed values (Fig. 5).

In order to determine the width of a continuous water tree l_a used in the computational thermal step current model $I_c(t)$, it was assumed that the water tree's cross section area is equal to the sum of areas corresponding to all the individual water trees from a cross section of a power cable, with these parameters L_m, D_m and c_{wtm}, resulting the following equation:

$$l_a = \frac{n_{wt} \cdot L_m \cdot D_m}{2\pi r_i}, \tag{8}$$

where $n_{wt} = c_{wtm} \cdot \pi\, r_i$ represents the average number of water trees in the cross section.

The thickness of the layer corresponding to the space charge was considered 35 % higher than those of l_a ($l_s = 1.35\ l_a$). The values for l_a and l_s corresponding to a water tree with a known length of $L_m = 370$ μm and a variable diameter D_m are presented in the Table 3.

Table 3

Values of l_a and l_s for water trees with a variable diameter D_m

($L_m = 370$ μm, $c_{wtm} = 1.27$ mm^{-1}, $n_{wt} = 2.7$)

D_m [μm]	110	200	300	400	500	600	787
l_a [μm]	52	111	140	188	235	282	370
l_s [μm]	70	150	189	254	317	381	500

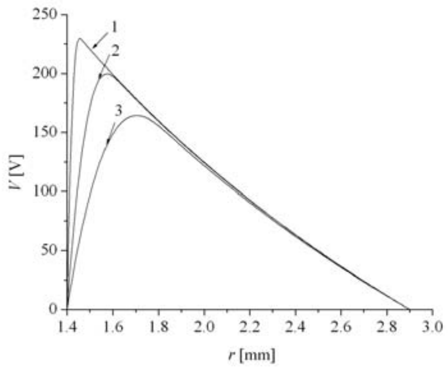

Fig. 6 – Variation of the residual electric potential V on r-coordinate for water trees with $L_m = 370$ μm, $c_{wtm} = 1.27$ mm^{-1} and $D_m = 110$ μm (1), $D_m = 400$ μm (2) and $D_m = 790$ μm (3).

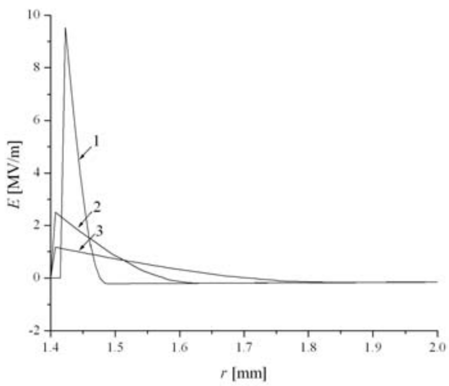

Fig. 7 – Variation of the residual electric field E on r-coordinate for water trees, with $L_m = 370$ μm, $c_{wtm} = 1.27$ mm^{-1} and $D_m = 110$ μm (1), $D_m = 400$ μm (2) and $D_m = 790$ μm (3).

In Fig. 6 and 7, the electric potential V and residual electric field E variations with r – coordinate are presented for water trees with $c_{wtm} = 1.27$ mm^{-1} and $L_m =$ = 370 μm. It can be observed that the electric potential has maximum values in the treed areas (in the vicinity of the inner semiconductor), areas where the charge layer l_s is situated. The increase of D_m values (thus of l_a, Table 3) leads to a decrease in the electric potential's maximum values and the displacement of these values towards the inside of the insulation (Fig. 6). This variation can be explained by an increase in the space charge layer thickness l_s and a decrease in the values of ρ_{v0} (the current $I_c(t)$ remaining constant).

The electric field dependence on the r-coordinate has the maximum points also situated in the treed areas (Fig. 7). Along with the increase of D_m (respectively, l_a) the maximum values for E decrease, and the maximum points move towards the inner semiconductor layer (Fig. 7). This decrease is due to the reduction of the charge density's ρ_{v0} maximum values (in the vicinity of the inner semiconductor layer) as a consequence of the increase – with D_m – in the values for l_s (Table 3).

The increase in the values for water tree concentration c_{wtm} leads to a reduction in the maximum values of E (Fig. 8, curve 1). This result is in agreement with the results obtained in the case of the computation of the electrical field for a cable insulation that only has an individual water tree [6].

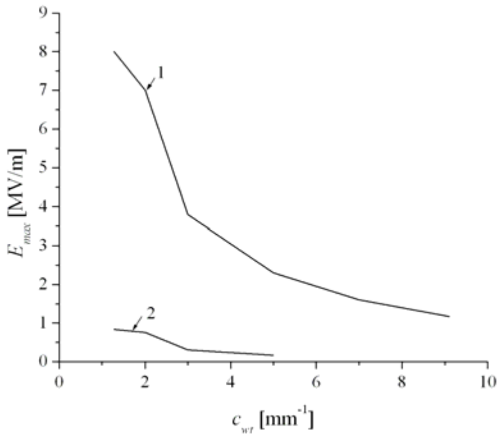

Fig. 8 – Variation of electric field E_{max} on trees concentration c_{wtm} for L_m = 370 μm and D_m = 110 μm (1) and L_m = 343 μm and D_m = 83 μm (2).

The decrease of the stress time of cables in electric field determines a reduction in the dimensions and concentration of water trees (Table 2). This leads to even lower values for the measured thermal step currents (Fig. 5) and, finally, to obtaining smaller values for l_a (8.8 μm) and l_s (12 μm). Thereby, the maximum values of the electric potential and of the residual electric field were considerably reduced (Fig. 8, curve 2).

It must be also noticed that the determination of the average ionic space charge density and the associated residual electric field based on the values of the measured thermal step current $I_m(t)$ may lead to important errors if the real dimensions of the individual water trees are not taken into account. Thereby, for the same curve $I_m(t)$ (dependent on the water trees dimensions and concentrations), the residual electric fields maximum values obtained by computation (with the COMSOL Multiphysics software) may vary with over one size order (Fig. 8). If the ageing time τ increases from 500 h to 1,000 h, the water tree density increases from 0.31 to 1.27 mm^{-1}, but their length increase with only 11 % (their growth rate being lower, Table 2).The decrease of the water trees growth velocity shows that in the curve $L_m(\tau)$ [1] the area of slow propagation was reached and a breakdown of the sample is soon possible.

The growth of water trees in polymer cable insulations also leads to an accumulation of ionic space charge which generates residual electric fields of relatively high intensities (10 MV/m, Fig. 7). These fields facilitate the appearance of partial discharges and electrical trees that may initiate a process of premature breakdown of cables insulations, even after the voltage is turn off.

6. CONCLUSIONS

The rise of the operation time of power cables leads to the increase in the dimensions and concentrations of water trees, and, consequently, of the ionic space charge in the insulations. The concentration and dimensions of water trees strongly influence the values and repartition of the residual electric field. Thereby, its maximum values increase along with the average length of the water trees, but decrease along with the increase in diameter and concentration.

The existence of some water trees with high lengths and small concentrations facilitates the appearance of high value residual electric fields (up to 10 MV/m), when partial discharges and electrical trees are initiated (3 MV/m). These may lead to premature breakdowns of power cable insulations.

Received on January 26, 2010

REFERENCES

1. L.A. Dissado, J.C. Fothergill, *Electrical Degradation and Breakdown in Polymers*, Peter Peregrinus Ltd., London, United Kingdom, 1992.
2. R. Ross, *Inception and Propagation Mechanisms of Water Treeing*, IEEE Transactions on Dielectrics and Electrical Insulation, **5**, *5*, pp. 660–680 (1998).
3. Oana Visata, *Influence des Arborescences d'eau sur les propriétés diélectriques des polymères*, PhD Dissertation, UPB-UJF, Bucharest, 2001.
4. P. Notingher jr., A. Toureille, S. Agnel, J. Castellon, *Determination of Electric Field and Space Charge in the Insulation of Power Cables With the Thermal Step Method and a New Mathematical Processing*, IEEE Trans. on Industry Applications, **45**, *1*, pp. 67–74 (2009).
5. Cristina Stancu, *Caractérisation de l'état de vieillissement des isolations polymères par la mesure des arborescences et de charges d'espace*, PhD Thesis, UPB-UM2, 2008.
6. Cristina Stancu, P.V. Notingher, F. Ciuprina, P. Notingher jr, S. Agnel, J. Castellon, A. Toureille, *Computation of the Electric Field in Cable Insulation in the Presence of Water Trees and Space Charge*, IEEE Transactions on Industry Applications, **45**, *1*, pp. 30–49 (2009).
7. Cristina Stancu, P.V. Notingher, P. Notingher jr, M. Plopeanu, *Electric Field Determination in Water Treed Samples Using the Thermal Step Method*, Journal of International Scientific Publications, Materials, Methods & Technologies, **3**, *1*, pp. 51–62 (2009).

8. Cristina Stancu, P. Notingher jr., P.V. Notingher, J. Castellon, S. Agnel, A. Toureille, U. Nilsson, A. Campus, D. Wald, *Water-Tree and Space Charge Characterization of Polyethylene Cable Insulation ac-Aged in Aqueous Environment*, Journal of Optoelectronics and Advanced Materials – Symposia, **1**, *5*, pp. 925–931 (2009).
9. A. Cernomorcenco, P. Notingher jr, *Application of the thermal step method to space charge measurements in inhomogeneous solid insulating structures: A theoretical approach*, Applied Physics Letters, **93**, pp. 192903 – 1 to 3 (2008).
10. T. Meissner, F. Wentz, *The complex dielectric constant of pure and sea water from microwave satellite observations*, IEEE Trans. Geoscience Remote Sensing, **42**, pp. 1836–1849 (2004).
11. V. Svorcik, D. Erkt, V. Rybka, J. Liptak, V. Hnatowicz, *Permittivity of polyethylene and polyethylene-terephtalate*, Journal of Materials Science Letters, **19**, pp. 1843–1845 (2000).